

Toward Prediction of Magnetic Properties in Layered Vanadyl Phosphonates: Correlation of Magnetic Exchange with the Hammett σ Parameter

Jean Le Bideau, Dimitris Papoutsakis, James E. Jackson,* and Daniel G. Nocera*

Contribution from the Department of Chemistry and Center for Fundamental Materials Research, Michigan State University, East Lansing, Michigan 48824

Received July 18, 1996[⊗]

Abstract: The magnetic properties of the layered vanadyl phosphonates (LVPs) $\text{VO}(\text{O}_3\text{PC}_6\text{H}_4\text{-X})\cdot n\text{H}_2\text{O}$ ($\text{X} = p\text{-NO}_2$, $m\text{-F}$, $p\text{-Cl}$, $p\text{-F}$, H , $p\text{-CH}_3$) have been investigated. In the isostructural $n = 1$ series ($\text{X} = p\text{-NO}_2$, $m\text{-F}$, $p\text{-F}$, H), the paramagnetic d^1 vanadyl centers are coupled via the O–P–O pathways of $\text{V}(\text{OPO})_2\text{V}$ chair-like subunits. The magnetic properties of these LVPs can be systematically controlled by modification of the P atom's electronic environment via variations of the X group in the aryl pendant. The simple paramagnetism of the LVP featuring the strong electron withdrawing substituent $\text{X} = p\text{-NO}_2$ gives way to increasing antiferromagnetic coupling between the V^{IV} centers as the electron-donating ability of X is increased. Consistent with a chair-like $\text{V}(\text{OPO})_2\text{V}$ exchange pathway between pairs of vanadyl centers, the temperature-dependent magnetic susceptibility data fit a Bleaney–Bowers dimer model. When the substituent is large, as is the case for the $p\text{-Cl}$ and $p\text{-CH}_3$ species, a structurally different class of LVPs is obtained, in which $n = 1.5$. In this case, the contribution of the O–P–O linkage is overwhelmed by the presence of the more direct exchange pathway of vanadyl centers through μ^2 -bridging oxygens of a $\text{V}(\mu^2\text{-O})_2\text{V}$ dimer, obviating the effects of electronic variations in the phosphonate bridge. Our results show that magnetic coupling correlates with a simple measure of electronic perturbation of the exchange pathway in LVPs, implying that such interactions can be tuned using the traditional tools of physical organic chemistry.

Introduction

In spite of formidable growth in the field of molecular magnetism, a need remains for general structural and electronic benchmarks to guide the synthetic chemist in the rational design of magnetic materials. Recent discoveries of exquisite assemblies of paramagnetic building blocks into materials with novel magnetic properties^{1–4} have only served to make this need more poignant. Significant steps toward structural understanding are seen in the correlation of magnetic coupling with the geometrical parameters in molecular building blocks. Nowhere is this approach better illustrated than in the well-studied $d^9\text{-}d^9$ $\text{Cu}(\mu^2\text{-OH})_2\text{Cu}$ dimers, in which the relationship between J coupling and the Cu-O-Cu angle has been mapped out in elegant detail.⁵ These ideas have been extended to $\text{VO}(\mu^2\text{-OR})_2\text{-VO}$ dimers, a series with $d^1\text{-}d^1$ electron counts,⁶ and to other oxo-bridged bimetallic complexes.^{7–9} Dimers of the $\text{M}(\mu^2\text{-OR})_2\text{M}$ class have also served to illuminate basic electronic questions. The isostructural $d^9\text{-}d^n$ $\text{Cu}(\mu^2\text{-OR})_2\text{M}$ ($\text{M} = \text{VO}$,

Fe, Ni, Cu) molecular complexes, where a dinucleating ligand template (derived from N,N' -(2-hydroxy-3-carboxybenzylidene)-ethylenediamine) enforces the pairwise relationship,¹⁰ have permitted examination within a unified framework of the relationship between orbital parentages and magnetic couplings. Yet a systematic understanding of the coupling between the same magnetic orbitals in an isostructural framework remains elusive. Such insight would allow the magnetic properties of materials to be analyzed in terms of fundamental chemical concepts familiar to molecular chemistry, and separate from simple geometrical issues.

Our strategy to define magnetic correlations in an isomorphous and isoelectronic family of compounds is to exploit the structural control available in self-assembled extended arrays.^{11–14} In particular, the layered vanadyl phosphonates (LVPs) $\text{VO}(\text{O}_3\text{-PC}_6\text{H}_4\text{-X})\cdot n\text{H}_2\text{O}$ allow structural orthogonalization of substituent variations from the magnetic network. These crystalline compounds are composed of tetragonal d^1 $\text{V}=\text{O}$ paramagnetic centers linked by phosphonate O–P–O bridges. Our studies of alkali metal intercalated VOPO_4 ,¹⁵ as well as earlier work on VOSO_4 ,¹⁶ $\text{VOHPO}_4\cdot 4\text{H}_2\text{O}$,¹⁷ and related systems,¹⁸ have established the magnetic coupling role of the V-O-P-O-V

[⊗] Abstract published in *Advance ACS Abstracts*, February 1, 1997.

- (1) Kahn, O. *Molecular Magnetism*; VCH: Weinheim, 1993.
- (2) (a) Miller, J. S.; Epstein, A. J. In *Materials Chemistry: An Emerging Discipline*; Adv. Chem. Ser. No. 245; American Chemical Society: Washington, DC, 1995; p 161. (b) *Proceedings on the Conference on Molecule-based Magnets*; Miller, J. S., Epstein, A. J., Eds.; Gordon and Breach: Amsterdam, 1995; Mol. Cryst. Liq. Cryst. Vol: 271–274. (c) Miller, J. S.; Epstein, A. J. *Angew. Chem., Int. Ed. Engl.* **1994**, *33*, 385.
- (3) Gatteschi, D. *Adv. Mater.* **1994**, *6*, 635.
- (4) *Research Frontiers in Magnetochemistry*; O'Connor, C. J., Ed.; World Scientific: Hong Kong, 1993.
- (5) Hatfield, W. E. In *Magneto-Structural Correlations in Exchange Coupled Systems*; Willett, R. D., Gatteschi, D., Kahn, O., Eds.; NATO ASI Series; Reidel: Dordrecht, 1985.
- (6) Plass, W. *Angew. Chem., Int. Ed. Engl.* **1996**, *35*, 627.
- (7) Gorun, S. M.; Lippard, S. J. *Inorg. Chem.* **1991**, *30*, 1625.
- (8) Niemann, A.; Bossek, U.; Wieghardt, K.; Butzlaff, C.; Trautwein, A. X.; Nuber, B. *Angew. Chem., Int. Ed. Engl.* **1992**, *31*, 311.
- (9) Nanda, K. K.; Thompson, L. K.; Bridson, J. N.; Nag, K. *J. Chem. Soc., Chem. Commun.* **1994**, 1337.

- (10) (a) Journaux, Y.; Kahn, O.; Morgenstern-Badarau, I.; Galy, J.; Jaud, J. *J. Am. Chem. Soc.* **1983**, *105*, 7585. (b) Kahn, O.; Galy, J.; Journaux, Y.; Morgenstern-Badarau, I. *J. Am. Chem. Soc.* **1982**, *104*, 2165. (c) Morgenstern-Badarau, I.; Rerat, M.; Kahn, O.; Jaud, J.; Galy, J. *Inorg. Chem.* **1982**, *21*, 3050.

- (11) Lehn, J.-M. *Supramolecular Chemistry*; VCH: Weinheim, 1995.
- (12) *Supramolecular Architecture*; Bein, T., Ed.; ACS Symp. Ser. No. 499; American Chemical Society: Washington, DC, 1992.
- (13) (a) Whitesides, G. M.; Simanek, E. E.; Mathias, J. P.; Seto, C. T.; Chin, D. N.; Mammen, M.; Gordon, D. M. *Acc. Chem. Res.* **1995**, *28*, 37. (b) Whitesides, G. M.; Mathias, J. P.; Seto, C. T. *Science* **1991**, *254*, 1312.
- (14) Desiraju, G. R. *Angew. Chem., Int. Ed. Engl.* **1995**, *34*, 2311.
- (15) Papoutsakis, D.; Jackson, J. E.; Nocera, D. G. *Inorg. Chem.* **1996**, *35*, 800.
- (16) Lezama, L.; Villeneuve, G.; Marcos, M. D.; Pizarro, J. L.; Hagenmuller, P.; Rojo, T. *Solid State Commun.* **1989**, *70*, 899.

link in the form of a $V(OPO)_2V$ chair framework. The LVPs retain the key $V(OPO)_2V$ chairs, but permit modification of the P atom's electronic environment via variations in the pendant aryl group. Because the organic pendants project into the interlayer region, substituent variations (out-of-plane) are orthogonal, and hence structurally isolated, from the (in-plane) magnetically active V, O, P layers. Substituent effects on magnetism should then be purely due to electronic perturbations. To exploit these characteristics, we have synthesized and characterized five new substituted $VO(O_3PC_6H_4-X)\cdot nH_2O$ LVPs ($X = p\text{-NO}_2, m\text{-F}, p\text{-F}$ for $n = 1$ and $p\text{-Cl}, p\text{-CH}_3$ for $n = 1.5$). The isostructural systems with $n = 1$, which include the known parent ($X = H$),¹⁹ show systematic variations in magnetic coupling as a function of the phosphonate pendants' donor/acceptor properties, as characterized by Hammett σ values.^{20,21} These results show that magnetic coupling correlates with a simple measure of the electronic perturbation in the exchange pathway between vanadyl centers thereby pointing the way to predictable magnetic behavior.

Experimental Section

Materials. Nitrophenylphosphonic acid was prepared from nitrophenyldiazonium fluoroborate as described by Doak and Freedman.²² Other phosphonic acids were made following the procedure given by Tavs.²³ Phenyl-substituted vanadyl phosphonates were prepared from V_2O_5 and phosphonic acid in H_2O by hydrothermal reaction in a 23-mL bomb filled to 18% volume at 220 °C for 5 days. The vanadium to phosphorus ratio was 1:2. Unsubstituted vanadyl phenylphosphonate, $VO(O_3PC_6H_5)\cdot H_2O$, was prepared by reacting 182 mg of V_2O_5 (98%), 150 mg of V_2O_3 (99%), and 1264 mg of phosphonic acid in 16.8 mL of water at 220 °C for 5 days. Products were isolated by vacuum filtration and washed repeatedly with water and ethanol and air dried overnight. The $VO(O_3PR)\cdot H_2O$ materials were obtained as green microcrystals whereas blue microcrystalline materials were isolated for the $VO(O_3PR)\cdot 1.5H_2O$ layer framework. Chemical analyses are as follows. Calcd. (Found), $VO(O_3PC_6H_5)\cdot H_2O$: V, 21.16 (21.24); P, 12.86 (12.66); C, 29.87 (29.84). Calcd. (Found), $VO(O_3PC_6H_4-p\text{-NO}_2)\cdot H_2O$: V, 17.81 (17.53); P, 10.83 (10.78); C, 25.20 (24.20); N, 4.90 (4.96). Calcd. (Found), $VO(O_3PC_6H_4-p\text{-F})\cdot H_2O$: V, 19.67 (19.02); P, 11.96 (11.51); C, 27.82 (28.78); F, 7.33 (7.33). Calcd. (Found), $VO(O_3PC_6H_4-p\text{-Cl})\cdot 1.5H_2O$: V, 18.49 (18.86); P, 11.24 (11.14); C, 26.16 (25.56); Cl, 12.87 (12.33).

Methods and Instrumentation. Infrared spectra were recorded on a Nicolet 740 FTIR spectrometer. A KBr beam splitter/DTGS-KBr detector was employed for the solid KBr pellet samples prepared, and an average of 32 scans was used for data collection. Powder X-ray diffraction patterns were recorded by using the Cu $K\alpha$ line (35 kV, 35 mA) of an INEL system equipped with a CPS 120 detector. To reduce preferred orientation problems associated with layered materials, the compounds were mounted in a capillary tube. Thermogravimetric analysis (TGA) was performed on Shimadzu TGA-50 under nitrogen at a 5 °C/min heating rate.

Electron paramagnetic resonance spectra of LVPs were measured by using a Bruker ER 200D X-band spectrometer equipped with an Oxford ESR-9 liquid helium cryostat. Magnetic fields were measured with a Bruker ER 035M gaussmeter, and the microwave frequency was measured with a Hewlett-Packard 5245L frequency counter. Magnetic susceptibilities were determined using a SQUID susceptometer (Quantum Design MPMSR2 susceptometer) within the 2 to 300

(17) Beltrán-Porter, D.; Beltrán-Porter, A.; Amorós, P.; Ibáñez, R.; Martínez, E.; Le Bail, A.; Ferey, G.; Villeneuve, G. *Eur. J. Solid State Inorg. Chem.* **1991**, *28*, 131.

(18) Linde, S. A.; Gorbunova, Y. E.; Lavrov, A. V.; Kustnetsov, Y. G. *Dokl. Akad. Nauk SSSR* **1979**, *224*, 1411.

(19) Huan, G.; Jacobson, A. J.; Johnson, J. W.; Corcoran, E. W., Jr. *Chem. Mater.* **1990**, *2*, 91.

(20) Nagarajan, K.; Shelly, K. P.; Perkins, R. R.; Stewart, R. *Can. J. Chem.* **1987**, *65*, 1729.

(21) Grabiak, R. C.; Miles, J. A.; Schwenzler, G. M. *Phosphorus Sulfur* **1980**, *9*, 197.

(22) Doak, G. O.; Freedman, L. D. *J. Am. Chem. Soc.* **1951**, *73*, 5658.

(23) Tavs, P. *Chem. Ber.* **1970**, *103*, 2428.

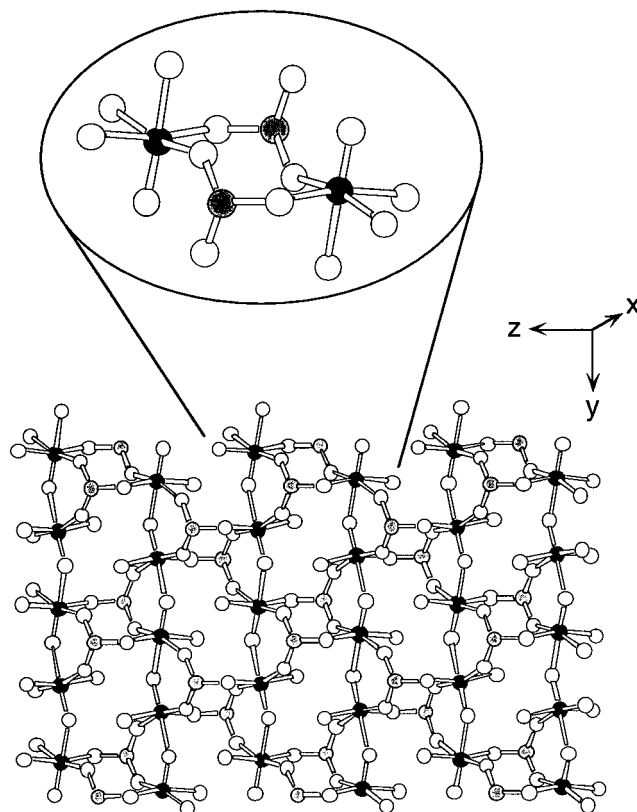


Figure 1. In-plane segment of the $VO(O_3PC_6H_4-X)\cdot H_2O$ ($X = p\text{-NO}_2, m\text{-F}, p\text{-F}$, and H) structure type (ref 19). The blow-up shows the chair-like $V(OPO)_2V$ subunits through which magnetic coupling occurs. The vanadium, phosphorus, and oxygen atoms are represented by black, gray, and white balls, respectively.

K temperature regime. The data were corrected for the diamagnetic contribution of the sample holder and for the diamagnetism of the compound, calculated using Pascal's constants.

Results and Discussion

The X-ray structure of the prototype LVP, $VO(O_3PC_6H_5)\cdot H_2O$ (i.e. $X = H$ above), has been reported by Jacobson, Johnson, and co-workers.¹⁹ Alternating inorganic and organic strata comprise respectively distorted octahedral vanadium and tetrahedral phosphorus oxide subunits, and phosphonate phenyl groups that converge in a bilayer arrangement from adjacent oxide layers. A view perpendicular to the layer plane is shown in Figure 1. Within the oxide layer, pairs of paramagnetic vanadyl centers are joined via chair-like $V(OPO)_2V$ links (see Figure 1), analogous to those we have recently discussed in the alkali metal intercalated $VOPO_4$ systems;¹⁵ these chair subunits are then stacked together, forming $V=O\cdots V=O$ chains. Based on powder X-ray diffraction, IR spectra (Table 1), and TGA, the fluoro and nitro compounds ($X = p\text{-F}, m\text{-F}$, and $p\text{-NO}_2$) are isostructural with the parent ($X = H$). The b and c cell parameters, which describe the inorganic layer, are similar as expected for an isostructural LVP series. It is the a dimension and hence the interlayer (or d) spacing that varies due to X substitution on the phenyl ring; d spacings derived from the a cell parameters of Table 1 are 14.14, 14.17, 14.18, and 15.13 Å for $X = H, p\text{-F}, m\text{-F}$, and $p\text{-NO}_2$, respectively.²⁴ Infrared spectra for the four are qualitatively similar,²⁵ with sharp $V=O$ and $P-O$ bands that show small variations in stretching

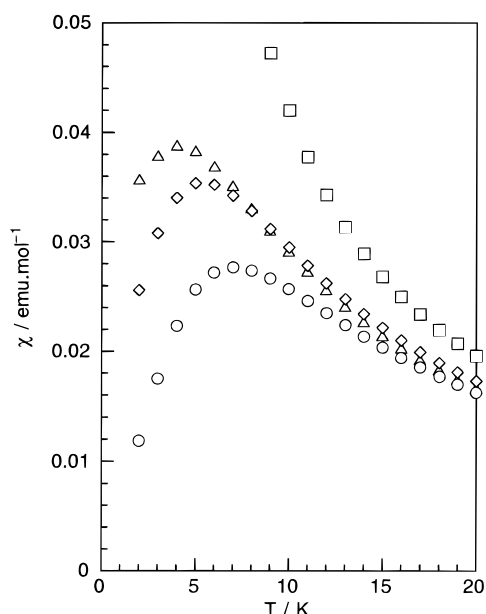
(24) Variation of the interlayer distance does not appear to modify magnetic properties of layered metal phosphonates (Le Bideau, J.; Payen, C.; Bujoli, B. *C. R. Acad. Sci. Paris* **1995**, *320*, 141).

(25) Infrared spectra for the LVPs described here are included in Supporting Information, along with tables of powder X-ray diffraction lines for the three (new) substituted cases.

Table 1. Selected Structural, Vibrational, and Magnetic Data for VO(O₃PC₆H₄-X)·H₂O LVPs and Hammett σ Values for C₆H₄-X

	C ₆ H ₅	C ₆ H ₄ - <i>p</i> -F	C ₆ H ₄ - <i>m</i> -F	C ₆ H ₄ - <i>p</i> -NO ₂
<i>a</i> (Å)	28.50	28.59(3)	28.60(1)	30.50(5)
<i>b</i> (Å)	7.18	7.16(1)	7.15(1)	6.98(1)
<i>c</i> (Å)	9.42	9.45(1)	9.44(1)	9.55(2)
β (deg)	97.1	97.6(1)	97.5(1)	97.1(1)
<i>d</i> -spacing (Å)	14.14	14.17	14.18	15.13
$\nu_{V=O}$ (cm ⁻¹)	883	885	882	895
ν_{P-O} (cm ⁻¹)	1046	1044	1043	1051
<i>C</i> (emu·K mol ⁻¹) ^a	0.360	0.359	0.368	0.374
Θ (K) ^a	-2.3	-1.1	-3.5 ^d	-0.1
μ_{eff} (μB) ^a	1.70	1.69	1.72	1.73
$T(\chi_{\text{max}})$ (K)	7	5.5	4.0	0
<i>J/k</i> (K) ^b	-5.5	-4.5	-3.3	0
σ^c	0.0	0.15	0.34	0.81

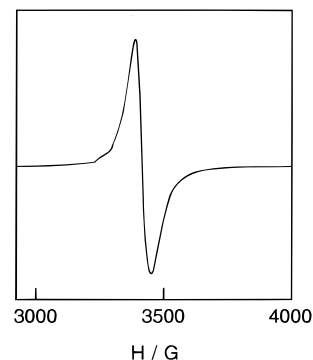
^a Determined over the range $T = 50$ – 100 K. ^b From Bleaney–Bowers fit (eq 2) to data over the range $T = 2$ – 100 K. ^c Substituent constants from: March, J. *Advanced Organic Chemistry*, 4th ed.; John Wiley & Sons: New York, 1992. ^d This low value is inaccurate due to curvature in the $1/\chi$ vs T plot in the 50–100 K temperature region of interest.

**Figure 2.** Plot of χ vs T for VO(O₃PC₆H₄-X)·H₂O (X = *p*-NO₂ (square), *m*-F (triangle), *p*-F, (diamond), and H (circle)) showing the broad paramagnetic maxima for the latter three.

frequencies. The TGA results²⁶ of 1 H₂O per formula unit further solidify the assignment of the *p*-F, *m*-F, and *p*-NO₂ phenylphosphonates to the same structural class as the parent VO(O₃PC₆H₅)·H₂O.

Figure 2 shows the temperature-dependent magnetic susceptibilities for the four LVPs with X = *p*-NO₂, *m*-F, *p*-F, and H. The LVP (X = *p*-NO₂) is a simple paramagnet, exhibiting Curie behavior with a negligible Weiss constant of -0.1 K. Conversely, the downturns seen in the data for X = H, *m*-F, and *p*-F indicate intralayer antiferromagnetic couplings between the V^{IV} centers. Although no indication of long-range magnetic ordering can be found down to 2 K, the broad paramagnetic maximum observed in Figure 2 for these compounds is characteristic of low-dimensional antiferromagnetic interactions. The magnetic data for the four compounds are summarized in Table 1. The values of the Curie constants *C*, obtained from the high temperature data, are all close to the spin-only value

(26) There are three types of vanadyl phosphonate structure, each with a different water content ($n = 1.0, 1.5, 2.0$); see refs 19 and 30. Thus, besides the structurally characteristic IR spectra, and X-ray powder diffraction data, the water content provides additional definitive support for structural assignments.

**Figure 3.** EPR spectrum of VO(O₃PC₆H₄-*p*-NO₂)·H₂O (the microwave frequency was 9.450 GHz and $g = 1.98$).

of 0.367(4) indicating good agreement between our chemical analyses and magnetic measurements. This spin-only value was obtained from the Curie expression (eq 1, where *N* is Avogadro's

$$C = \frac{Ng^2\mu_B^2}{3k}S(S+1) = \chi T \quad (1)$$

number, μ_B is the Bohr magneton, and *k* is the Boltzmann constant) by using the value of $g = 1.98(1)$ determined from our EPR measurements for the four LVPs, which showed essentially identical spectra. A representative example, shown in Figure 3, is broadened and symmetrical like those seen in the d¹ dimer-containing VOHPO₄ layers¹⁷ and related systems.^{16,27}

Owing to the highly coupled network within the layers (Figure 1), a complete model for the magnetism in these systems is difficult to derive. Nevertheless, the dominant magnetic subunits in these systems are thought to be the chair-like V(OPO)₂V exchange pathways described above; the V=O···V=O pathways are orthogonal to the d_{xy} magnetic orbital and accordingly coupling through the oxo bridges does not appear to be significant.²⁸ Thus, as a first approximation, using a Heisenberg Hamiltonian $H = -2JS_xS_y$, we estimate the magnetic interaction with a Bleaney–Bowers model for dimers,²⁹

$$\chi = (1-f) \left\{ \frac{Ng^2\mu_B^2}{kT} \cdot \frac{1}{3 + \exp(-2J/kT)} \right\} + f \frac{C}{T} \quad (2)$$

where *f* is the amount of paramagnetic impurities taken as isolated V^{IV} ions, and $g = 1.98$. The *J/k* values of Table 1 were obtained from fits of eq 2 with $f = 0.05, 0.1,$ and 0.0 for X = H, *p*-F, and *m*-F, respectively.

The LVPs with X = Cl and CH₃ cannot be included in the correlation of Table 1 and Figure 2 (see below) because they fall outside the above structural group; instead they are isostructural with the alkyl phosphonates VO(O₃PR)·1.5H₂O (R = CH₃, C₂H₆, *n*-C₃H₇) as revealed by TGA and IR.²⁵ From a partial structure solution of VO(O₃PCH₃)·1.5H₂O,³⁰ these compounds appear to have the same layered framework as VO-(HOPO₃)·0.5H₂O,³¹ in which vanadyl centers interact directly through μ^2 -bridging oxygens of a V(μ^2 -O)₂V dimer (see Figure 4). We believe the switchover in structural motif for the X = Cl and CH₃ cases results from the steric bulk of the substituents; H, F, and NO₂ are small, while CH₃ and Cl are both thicker than an aryl ring. Variable-temperature susceptibility data for

(27) Shin, Y.-g. K.; Nocera, D. G. *J. Am. Chem. Soc.* **1992**, *114*, 1264.(28) Beltrán-Porter, D.; Amorós, P.; Ibáñez, R.; Le Bail, A.; Ferey, G.; Villeneuve, G. *Solid State Ionics* **1989**, *32*, 57.(29) Carlin, R. L. *Magnetochemistry*; Springer-Verlag: Berlin, 1986.(30) Huan, G.; Johnson, J. W.; Brody, J. F.; Goshorn, D. P.; Jacobson, A. J. *Mater. Chem. Phys.* **1993**, *35*, 199.(31) Leonowicz, M. E.; Johnson, J. W.; Brody, J. F.; Shannon, H. F., Jr.; Newsam, J. M. *J. Solid State Chem.* **1985**, *56*, 370.

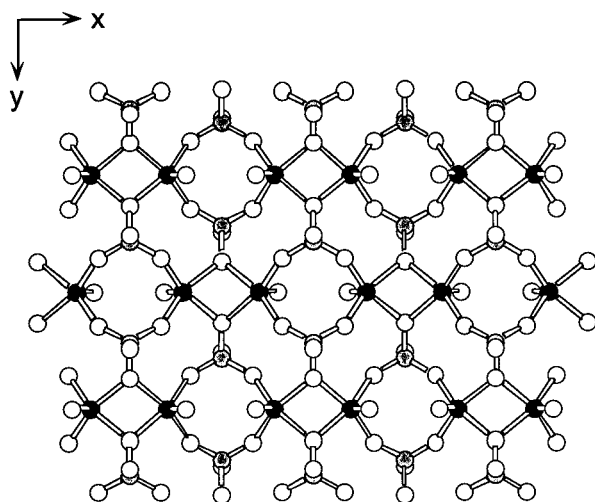


Figure 4. In-plane segment of vanadyl hydrogen phosphate hemihydrate,³¹ which is isostructural with the $\text{VO}(\text{O}_3\text{PC}_6\text{H}_4\text{-X})\cdot 1.5\text{H}_2\text{O}$ ($\text{X} = \text{Cl}, \text{CH}_3$) as described in ref 30. Vanadium, phosphorous and oxygen are represented by the black, gray, and white balls, respectively. The aromatic rings and the water oxygen have been omitted for clarity. The $\text{V}(\mu^2\text{-O})_2\text{V}$ dimer is the dominant magnetic pathway in this structure type.

these compounds show antiferromagnetic downturns, with $T(\chi_{\text{max}})$ values at 54 ($\text{X} = p\text{-Cl}$) and 58 K ($\text{X} = p\text{-CH}_3$), substantially higher than those seen in Figure 2, and consistent with the known stronger coupling ability of the $\text{V}(\mu^2\text{-O})_2\text{V}$ dimer magnetic pathway.²⁸ The Bleaney–Bowers-derived J/k values (-42 and -48 K, respectively) for these new aryl phosphonate systems are in the same range as those found in the alkyl phosphonate cases (-43 to -52 K for simple alkyl groups)³⁰ and in the vanadyl hydrogen phosphate hemihydrate (-43 K).¹⁷ With the stronger $(\mu^2\text{-O})_2$ bridge supplanting the $(\text{OPO})_2$ linkages in the Bleaney–Bowers dimers, the phosphonates are now mainly in the role of ligands about the VO centers, so the effects of substituent variations would be expected to be qualitatively different than for the $n = 1$ series.

In the aryl phosphonate systems where the O–P–O pathway dominates exchange between vanadyl centers, the magnetic coupling responds to variations in Hammett σ values which, in turn, reflect the electronic environment at the P atom. This constant is defined via the acidity of the benzoic acids $\text{X-C}_6\text{H}_4\text{-COOH}$ with X in the meta or para position on the phenyl ring. The value of σ for the $p\text{-NO}_2$ group, for instance, is then the difference in $\text{p}K_{\text{a}}$ (acid strength) between parent and substituted benzoic acids [i.e. $\sigma = \text{p}K_{\text{a}}(\text{X}=\text{H}) - \text{p}K_{\text{a}}(\text{X}=p\text{-NO}_2)$]; the p -nitrobenzoic acid is more readily ionized (i.e. stronger, $\text{p}K_{\text{a}}$ lower) due to the electron-accepting ability of the NO_2 group, so σ is positive for such electron-withdrawing groups. The σ constants thus reflect composite resonance and inductive electron withdrawal along with dipole changes in the molecules. As seen in Figure 5, a plot of J/k vs σ is monotonic; for a simple linear fit, a slope of 6.8 is obtained. Other properties that depend on the electronic environment of phosphorus—specifically, the $\text{p}K_{\text{a}}$ values in aryl phosphonic acids²⁰ and ^{31}P NMR chemical shifts in the related aryl phosphonic dichlorides²¹—show linear correlations with σ , but it is less clear what to expect in the present case. A trend to weaker coupling with increasing σ seems sensible on simple frontier orbital grounds; as substituents become more electron withdrawing, the energy mismatch between phosphonate orbital energies and vanadyl d levels widens, leading to decreased

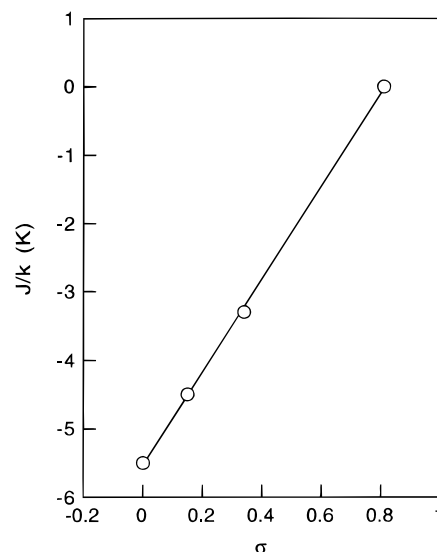


Figure 5. Plot of J/k vs σ for the four LVPs $\text{VO}(\text{O}_3\text{PC}_6\text{H}_4\text{-X})\cdot\text{H}_2\text{O}$ ($\text{X} = p\text{-NO}_2, m\text{-F}, p\text{-F}, \text{H}$).

interaction and hence coupling. Of course, a detailed electronic and structural explanation would require insights from numerous additional experiments and electronic structure calculations.

A previous report has attempted to link vanadyl–vanadyl J coupling with the Lewis acidity of intercalated metal cations in a series of MV_3O_7 ($\text{M} = \text{Ca}, \text{Cd}, \text{Sr}$) layered materials. The trend uncovered in this series agrees with our own; coupling becomes weaker as electron-withdrawing ability rises, due to increasing cation Lewis acidity or aryl substituent σ value. However, significant variations in intralayer V–O–V angles mar the strict correlation of the electronic effects with the chosen perturbation.³² In addition, the rather unusual g values reported from the magnetic susceptibility data fits cloud the interpretation further. Our ability to demonstrate a correlation of magnetism to a simple electronic perturbation rests on the dimensional separation between the magnetic network in the 2D layers and the structural effects of substituent variations orthogonal to the layers. It is satisfying that classical physical organic tools, long used to probe mechanistic issues and more recently applied to the study of spin couplings in molecular systems,^{33–35} can even shed light on magnetic interactions in extended materials such as the LVPs.

Acknowledgment. The financial support of the National Science Foundation (DMR-9311597) and the Center for Fundamental Materials Research at MSU is gratefully acknowledged.

Supporting Information Available: Infrared spectra of $\text{VO}(\text{O}_3\text{PC}_6\text{H}_4\text{-X})\cdot n\text{H}_2\text{O}$ LVPs ($\text{X} = p\text{-NO}_2, m\text{-F}, p\text{-F}, \text{H}$ for $n = 1$; Cl, CH_3 for $n = 1.5$) and $\text{VO}(\text{O}_3\text{PCH}_3)\cdot 1.5\text{H}_2\text{O}$ and tables of powder X-ray diffraction lines for $\text{VO}(\text{O}_3\text{PC}_6\text{H}_4\text{-}p\text{-F})\cdot\text{H}_2\text{O}$, $\text{VO}(\text{O}_3\text{PC}_6\text{H}_4\text{-}m\text{-F})\cdot\text{H}_2\text{O}$, and $\text{VO}(\text{O}_3\text{PC}_6\text{H}_4\text{-}p\text{-NO}_2)\cdot\text{H}_2\text{O}$ (3 pages). See any current masthead page for ordering and Internet access information.

JA9624836

(32) Liu, G.; Greedan, J. E. *J. Solid. State Chem.* **1993**, *103*, 139.

(33) Jang, S.-H.; Mitchell, C.; Jackson, J. E.; Kahr, B. *Mol. Cryst. Liq. Cryst.* **1995**, *272*, 147.

(34) West, A. P., Jr.; Silverman, S. K.; Dougherty, D. A. *J. Am. Chem. Soc.* **1996**, *118*, 1452.

(35) Adam, W.; Fröhlich, L.; Nau, W. M.; Korth, H.-G.; Sustmann, R. *Angew. Chem., Int. Ed. Engl.* **1993**, *32*, 1339.